nature communications

Article | Article in Press

https://doi.org/10.1038/s41467-026-79185-2

Building materials and emissions from rebuilding under increasing climate-driven flood hazards

Received: 15 February 2025

Accepted: 14 October 2026

Published online: 26 October 2026

Check for updates

Xiaoyang Zhong[1,2,3] ✉, Tomer Fishman[3], Timothy Tiggeloven[4,5], Yoav Peled[6], Yi Jin[7], Philip J. Ward[5,8] & Paul Behrens[3,9]

Floods threaten lives and infrastructure, while recovery and reconstruction require materials whose production generates greenhouse gas emissions. These material needs and emissions remain insufficiently quantified. Here we assess the impacts of riverine and coastal flooding on building materials across Europe under climate change and land subsidence. Baseline annual replacement demand is about 30 million tonnes of materials, generating about 9 million tonnes of carbon dioxide equivalent emissions. With flood protection maintained but not upgraded, both could increase more than tenfold by 2080 under a moderate emissions scenario, driven by coastal flooding. Impacts could be about 22% higher under a high emissions scenario. Cumulative replacement emissions over 2024–2080 under the moderate scenario could reach 4.0 billion tonnes of carbon dioxide equivalent, exceeding ten times Europe's annual building material production emissions in 2020. Increasing both mitigation and adaptation efforts is essential to reduce material losses, further emissions and human suffering.

Natural hazards present major risks to buildings and infrastructure globally. For instance, the 2022 deadly flooding in Pakistan destroyed more than 1.2 million houses, thousands of kilometres of road and hundreds of bridges[1]. Hurricane Maria left 400,000 houses damaged in Puerto Rico—one-third of the island's homes, many of which were informal and highly vulnerable structures[2]. The 2021 European floods damaged tens of thousands of homes across Germany, Belgium and the Netherlands[3], while the 2024 floods extended widespread destruction to Spain, Austria, Bosnia and beyond[4]. At least 642,000 homes have been damaged or destroyed in West and Central Africa due to flooding in 2024[5]. Meanwhile, over half of the building stock in the United States (US) is estimated to be at risk of potentially catastrophic natural hazards (i.e. earthquakes, floods, hurricanes, tornadoes and wildfires), with 1.5 million buildings located in hotspots of two or more hazards[6].

Floods represent the most prevalent and costly natural hazards globally[7], accounting for nearly half of the reported disasters in the past two decades[8] and over 70% of modelled hazard-related damages to transport infrastructures (among earthquakes, cyclones and floods)[9]. Global flooding is expected to intensify with climatic and land-use change (e.g. vegetation clearing and subsidence)[10–12], posing an increasing threat to buildings. In Europe, flood trends show marked regional heterogeneity, with some regions experiencing increased flood frequency while others see reductions due to changes in precipitation seasonality and snowmelt timing[13,14]. Flood impacts on buildings and materials may be particularly severe in regions where financial constraints limit flood protection, adaptation and

[1]Institute of Environment and Ecology, Tsinghua Shenzhen International Graduate School, Tsinghua University, Shenzhen, China. [2]International Institute for Applied System Analysis (IIASA), Laxenburg, Austria. [3]Institute of Environmental Sciences (CML), Leiden University, Leiden, The Netherlands. [4]Euro-Mediterranean Center on Climate Change (CMCC), Venice, Italy. [5]Institute for Environmental Studies, Vrije Universiteit Amsterdam, Amsterdam, The Netherlands. [6]Wildfowl & Wetlands Trust, Slimbridge, Gloucestershire, UK. [7]Institute of Industrial Economics, Jiangsu University, Zhenjiang, China. [8]Deltares, Delft, The Netherlands. [9]Oxford Martin School, University of Oxford, Oxford, UK. ✉e-mail: x.zhong@sz.tsinghua.edu.cn

recovery[15,16]. For example, in the UK, flooding risks are correlated with deprivation[17] and the lowest income earners often have very low rates of flood insurance[18].

These combined trends may cause substantial material losses due to post-flooding repairs and rebuilding. This results in further material-related environmental impacts, such as greenhouse gas (GHG) emissions, which further threaten national and global climate targets. Previous studies have explored flood risks on population[7,11,12,15,16,19] and the economy[11,19–26]. However, the physical building material requirements and embodied emissions associated with flood repair and reconstruction remain largely unquantified. This is in large part due to the limited availability of spatially explicit information on the composition and mass of building stocks and materials[27,28]. Recent advances in computational, digital and earth observation technologies now facilitate more precise and extensive mapping, opening new possibilities for such assessments[29,30].

Here, we estimate European building materials at risk of flooding hazards and GHG emissions from replacing damaged or destroyed buildings under climate change, land-use change and flood protection scenarios. We use two spatially explicit datasets: (1) a building material stocks map including six material types for residential and non-residential buildings[29]; and (2) inundation maps of riverine and coastal floods for different return periods, modelled for a baseline of 2010 and future climate change and land subsidence under moderate and high emissions pathways, represented by Representative Concentration Pathways (RCPs) 4.5 and 8.5, respectively, through 2080 (see 'Methods' for more details). We analyse the exposure of building materials to riverine and coastal flooding events, i.e. materials located in areas with inundation depth greater than 0. We then estimate the expected annual damage (EAD) of building materials by considering a range of 9 return periods (2, 5, 10, 25, 50, 100, 250, 500 and 1000 years) and damage probabilities given by a depth–damage function (see 'Methods' for more). We calculate the embodied GHG emissions of building materials for repairing and rebuilding using a life cycle assessment approach. Given the limited availability of information on flood protection measures at large spatial scales, we calculate current exposure and EAD based on the implementation of estimated subnational flood protection standards from a global database[31]. We then assess how material damage and embodied emissions change under future scenarios if flood protection infrastructure remains at their current heights.

Results

Building material exposure is concentrated in Western and Southern Europe

With current flood protection measures, ~9.5 Gt of building materials (9.4% of the total European building material stock) are exposed to 100-year return period riverine (9.4 Gt) or coastal (1.2 Gt) flooding events (Fig. 1). Italy, France, the Netherlands and Germany see significant exposure (each representing more than 1 Gt and over 10% of the European total), followed by Turkey, Spain and the UK. These nations have accumulated a large quantity of building stocks in coastal areas, large river basins or lowland areas. By mass, concrete is the most exposed to 100-year return period floods, accounting for ~80% of the total, followed by wood and steel, each accounting for nearly 8%.

The current EAD to building materials from riverine and coastal floods is ~29 Mt, with nearly 90% of the damage attributed to riverine flooding. France (4 Mt), Spain (3.8 Mt), Turkey (2.7 Mt) and Italy (2.5 Mt) are the most affected, each seeing estimated replacement equivalent demand exceeding 2 Mt. Replacing these materials using current manufacturing methods would result in GHG emissions of around 9 Mt CO_2eq across Europe, including 1.3 Mt CO_2eq for France, 1.2 Mt CO_2eq for Spain and 0.8 Mt CO_2eq for both Turkey and Italy.

Future flood damages are increasingly driven by coastal hazards

Climatic and land use conditions are likely to significantly shape the EAD in the coming decades. To explore the future exposure to flooding, we evaluate EAD impacts in a situation where protection measures are maintained but not increased (dyke heights are kept constant over time). Under RCP 4.5 and RCP 8.5 scenarios, combined with land subsidence, EAD from flooding is projected to rise nearly 8-fold in 2050 (for both RCPs) and more than 10- and 13-fold, respectively, by 2080 (Fig. 2). These changes result from a combination of declining riverine flooding damages (27% and 28% lower by 2080 under RCP4.5 and RCP8.5) and a sharp rise in coastal flooding damages, which are projected to increase nearly 100-fold and 124-fold, respectively, by 2080 (Fig. 2).

Regional damage trajectories diverge across Europe

Regional trends vary significantly (Fig. 3 and Supplementary Figs. 9, 10). In some parts of Europe, such as Greece, Spain and Turkey, the EAD from riverine flooding is projected to decline by more than half due to drying effects EAD by 2080 under RCP4.5. In contrast, several central and eastern European countries such as Estonia, Slovenia,

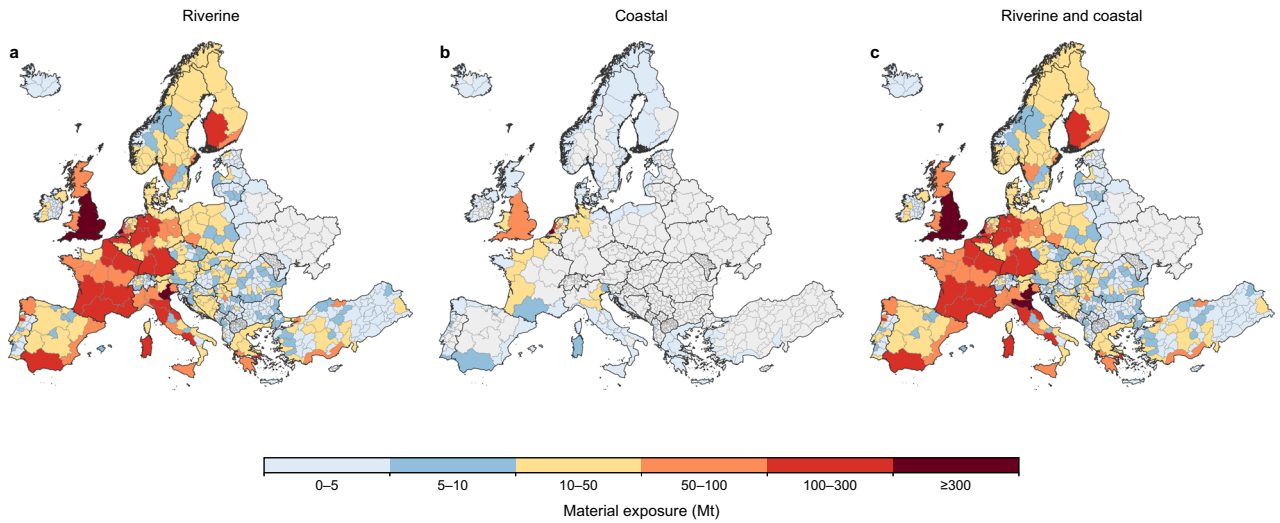


Fig. 1 | . Current building materials at risk of 100-year return period for riverine (**a**) and coastal (**b**) flooding events under current climatic conditions (reference year 2010). The combined riverine & coastal impacts are shown in (**c**). Spatial units are shown at the state and province level (GADM, 2024). Source data are provided as a Source Data file.

https://doi.org/10.1038/s41467-026-79185-2

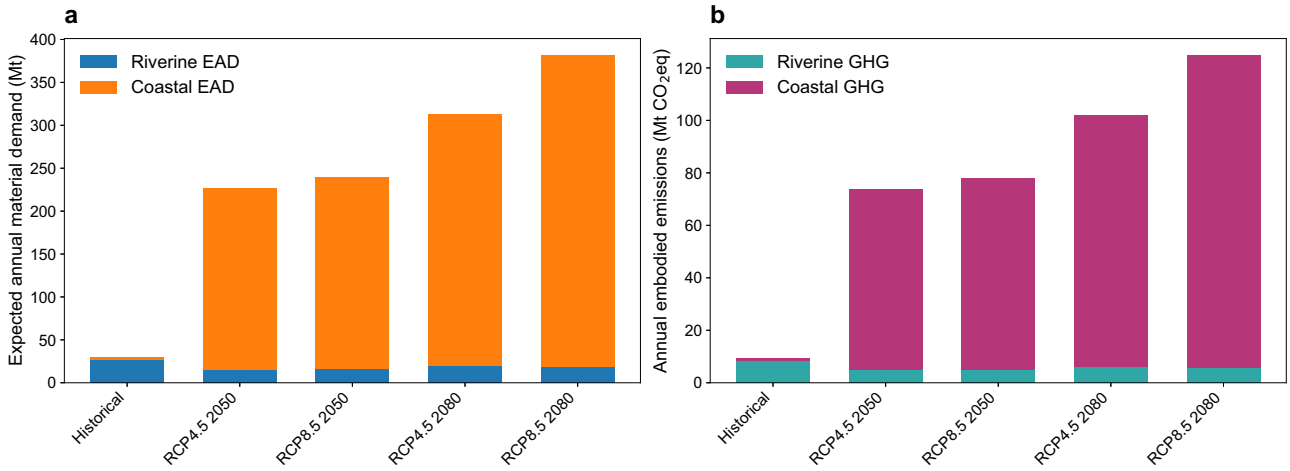


Fig. 2 | Expected annual replacement material demand and associated embodied emissions from flooding across Europe. a Expected annual damage (EAD), expressed as replacement material demand, from riverine and coastal flooding. **b** Associated embodied greenhouse gas (GHG) emissions from producing replacement materials. Results are shown for baseline conditions and future scenarios under Representative Concentration Pathways (RCPs) 4.5 and 8.5, with existing flood protection maintained but not upgraded. Material demand is expressed in million tonnes (Mt), and emissions in million tonnes of carbon dioxide equivalent (Mt CO_2eq). Source data are provided as a Source Data file.

Hungary, Croatia, Lithuania, Austria and Belgium see over twice the riverine flooding by 2080 in the same scenario. Coastal flooding damages, however, are expected to increase across almost all countries by 2080 under the same scenario. The Netherlands leads in absolute EAD increases (+270 Mt), followed by Germany, Belgium, Italy, France and the United Kingdom, all seeing increases of over 10 Mt. In relative terms, Belgium, Estonia, Lithuania, Germany and Croatia all see over 400-fold increases under RCP4.5 by 2080. Under RCP4.5, cumulative replacement material demand from riverine and coastal flooding in Europe is projected to reach 12.3 Gt over 2024–2080, with associated embodied emissions of approximately 4.0 GtCO_2eq. This is equivalent to approximately 12 times the annual emissions from building material production in Europe in 2020[32].

To assess the plausibility of our risk estimates, we compared modelled outputs against the observed July 2021 floods in Germany and Belgium—a 100–200 year return period event causing ~€33 billion in losses in Germany and ~€2.5 billion in Belgium[3,33]. Our model estimates a historical riverine EAD of ~1607 kt yr^{-1} for Germany and ~70 kt yr^{-1} for Belgium; at the 100-year return period, ~1021 Mt of building materials are exposed to riverine flooding in Germany, consistent with the scale of an event affecting tens of thousands of buildings across multiple federal states. Spatially, the model correctly identifies Rhineland-Palatinate and North Rhine-Westphalia as the highest-risk states in Germany, and assigns higher riverine EAD to Wallonia (~40 kt yr^{-1}) than Flanders (~29 kt yr^{-1}) in Belgium—both consistent with observed damage geography. An additional illustrative comparison between CEMS mapped flood evidence and the Aqueduct/GLOFRIS historical 100-year riverine hazard extent is provided in Supplementary Fig. 8. Full validation details, including a comparison with prior validation of the underlying flood hazard maps[25,34], are provided in Supplementary Discussion 2.

Discussion

Overall, flood protection standards will need upgrading in many regions, especially in those having a low level of current protection (such as North Macedonia and Romania) and those that have higher protection standards but see intensifying flooding hazards (such as the Netherlands and Belgium)[35]. The Netherlands has some of the best flood protection systems in the world that have largely reduced the risks, yet the floods of 2021 and 2024 have still resulted in material damage in the country[36]. Local geographic and socio-economic conditions need to be considered when implementing resource- and cost-effective flood protection measures that could range from hard physical barriers to nature-based solutions such as wetland restoration and flood detention ponds[37–39].

We find coastal flood damage increasing up to 100-fold under RCP4.5-2080 and 124-fold under RCP8.5-2080 relative to the historical baseline. This contrast between historical and future damage is primarily driven by projected sea-level rise (SLR). Under the historical climate, coastal flood protection standards (derived from FLOPROS) are largely adequate, resulting in low residual EAD (~2.9 Mt yr^{-1}). Under future scenarios, SLR progressively lowers the effective return period of coastal flood events: a flood that currently occurs once every 100 years may occur annually by mid-century in low-lying coastal areas, rapidly overwhelming existing protection infrastructure. The coastal flood maps used here[26] incorporate projected SLR from the Coupled Model Intercomparison Project Phase 5 (CMIP5) ensemble under RCP4.5 and RCP8.5, combined with dynamic storm surge modelling. Land subsidence, which further amplifies relative SLR in many European coastal regions, is also included. In contrast, riverine EAD shows a more modest and non-monotonic response to climate change: under RCP4.5-2050, European total riverine EAD decreases by ~40% relative to the historical baseline before partially recovering by 2080 (−27%). This counterintuitive pattern reflects the regionally heterogeneous response of river floods to climate change documented in the literature[14]: while some regions (e.g. southern and eastern Europe) experience increased flood frequency, others (e.g. northern and western Europe) see reduced flooding due to changes in precipitation seasonality and snowmelt timing. At the European aggregate level, these opposing regional trends partially cancel out, masking the increases that occur in specific sub-regions. It is also worth noting that a decline in aggregate riverine EAD does not necessarily mean individual flood events become less severe; precipitation may shift toward fewer but more intense episodes, with implications for infrastructure design and emergency preparedness.

In addition to strengthening flood protection measures, increasing flood hazards call for a systematic transformation in the built environment. Future urban planning and real estate investment decisions need to consider hazard hotspots and climate outcomes, avoiding urban planning failures such as building cities and homes in flood-prone areas as seen around the world in the past decades[6,40–42]. Incorporating flood zoning strategies[43] can help identify these

https://doi.org/10.1038/s41467-026-79185-2

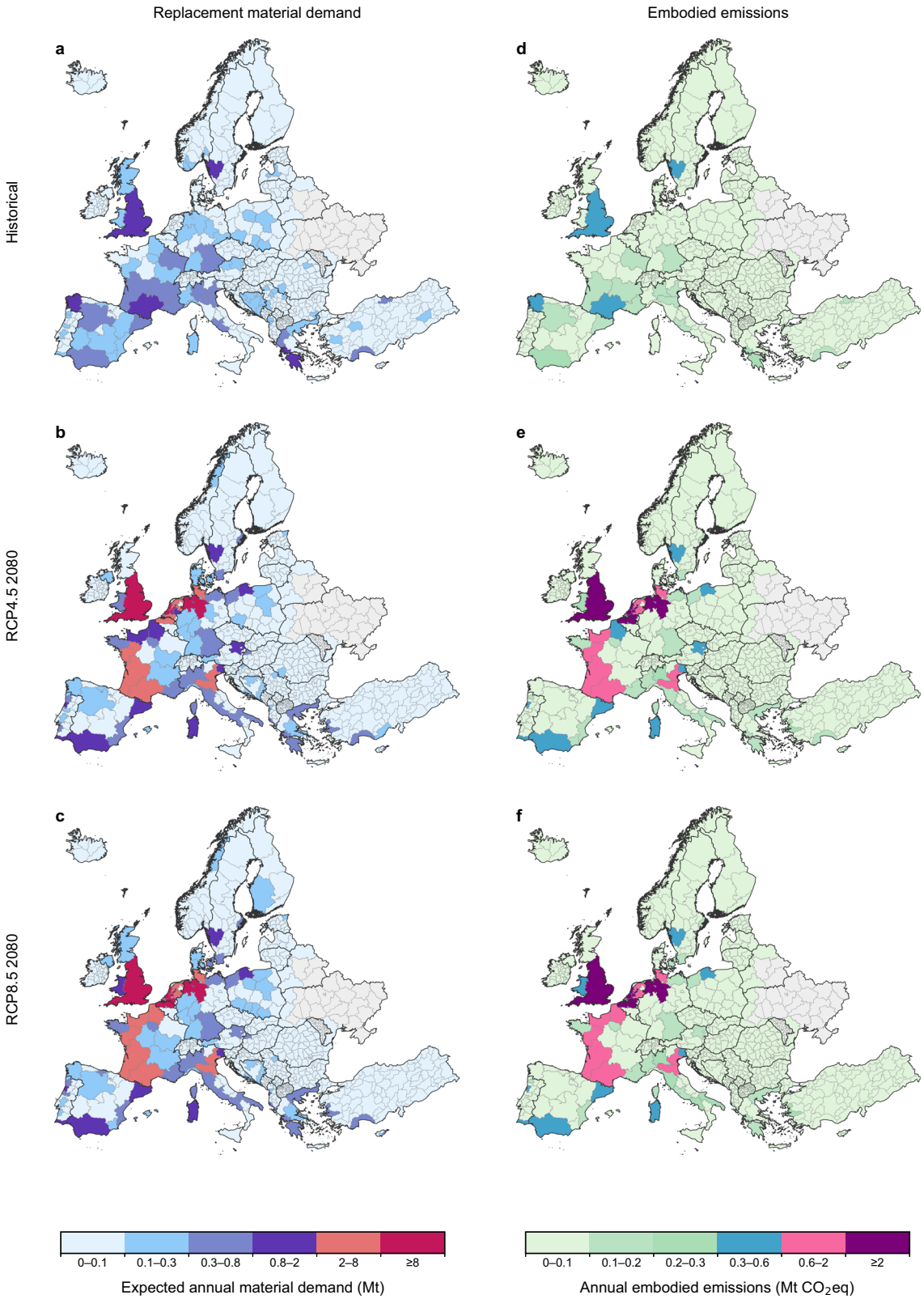


Fig. 3 | Expected annual damage (EAD) of building materials from riverine and coastal flooding hazards with estimated current flood protections (in Mt) and embodied greenhouse gas (GHG) emissions (in Mt CO_2eq). a–c EAD under the baseline (reference year 2010) and future climatic and land use conditions. **d–f** GHG emissions from the production of materials equivalent to the EAD across scenarios. Spatial units are shown at the state and province level (GADM, 2024). Source data are provided as a Source Data file.

hotspots, guide land use decisions, and ensure that high-risk areas are avoided for future developments.

The next generation of engineers will also need to build resilience into buildings during construction[44]. For example, structures designed to allow water entry and exit[45], foundations with higher depth and corrosion resistance[46], and waterproof materials[47] may help buildings survive flooding. Flood zoning data can inform site-specific designs, ensuring that structures in moderately risky zones are adapted to withstand flooding. Finally, flood-prone regions will need to develop waste management protocols to inventory and dispose of construction materials post-disaster[48,49]. Dedicated efforts are needed to reduce harm and pollution, accelerate reconstruction and rehabilitation, and make sure the right type of impacted materials can be sorted and recovered[49,50].

The framework we present can be used to map flooding impacts on building material stocks and embodied emissions on multiple scales. Analysing impacts in other regions of the world that currently do not have equivalent flood protection measures as Europe is essential. Future trends in building material stocks over time can be incorporated; this may include socioeconomic changes, which is especially important for rapidly developing countries where most homes are to be built by 2080. Another area for future work would be to estimate the net emission savings from flood protection measures. For example, the embodied emissions and materials of flooding protection infrastructure such as dikes could be assessed.

The embodied GHG emissions from flood-damaged building materials represent a growing but largely overlooked pressure on climate mitigation efforts. Under the historical climate, flood-related embodied emissions across Europe amount to ~9.2 $MtCO_2eq\ yr^{-1}$. Under RCP4.5-2080, this rises to ~102 $MtCO_2eq\ yr^{-1}$—equivalent to approximately 2.8% of total EU GHG emissions in 2022 (~3600 $MtCO_2eq\ yr^{-1}$). Under RCP8.5-2080, annual flood-related emissions reach ~125 $MtCO_2eq\ yr^{-1}$, a 13.6-fold increase relative to the historical baseline. Cumulatively over 2024–2080, flood-related embodied emissions are projected to reach 4.0 $GtCO_2eq$ under RCP4.5 and 4.5 $GtCO_2eq$ under RCP8.5, equivalent to approximately 23% and 26%, respectively, of the EU's estimated remaining carbon budget consistent with limiting warming to 1.5 °C. As such, these figures show that flood risk is not only a physical and economic challenge but also a threat to Europe's decarbonisation trajectory. Achieving the EU's climate neutrality goal by 2050 will require accounting for the emissions embodied in flood-driven reconstruction, alongside efforts to reduce operational building emissions. Flood protection investment and climate adaptation should therefore be recognised as integral components of emissions reduction strategy, not merely as separate resilience measures.

Data collection and methodological improvements are critical for advancing flood risk analysis. It is important to update and refine the data on flood protection measures. Currently, many studies either entirely overlook these measures[15,51] or base their estimates on indirect indicators such as income levels[9,31]. The development of flood risk assessment will also need to extend the depth–damage functions to not only consider monetary values but also incorporate physical material stocks, tailoring evaluations to reflect specific country and material characteristics more accurately. Finally, it is essential that future cost-benefit analyses of flood protection include the benefits of avoided GHG emissions, given the pressing need to manage our limited global emissions budget.

There are several limitations of this work. First, the flood hazard data used here have a spatial resolution of ~1 km (30″), which limits precision at the scale of individual settlements, particularly in narrow river valleys and small countries. Many European towns have urban footprints smaller than 2 km in diameter and are therefore represented by only one or two grid cells, or none at all; such settlements may be missed entirely. Our results are therefore most reliable when interpreted at the national or regional scale rather than for individual settlements. We also note that the FLOPROS protection standards used here are assigned at the sub-national administrative level and do not capture within-region variation in flood protection between urban centers and surrounding suburban or rural areas, where buildings may be more susceptible to flood damage. Higher-resolution flood products (e.g. at 100 m resolution) are increasingly available for Europe and would improve local accuracy, though continental-scale coverage at such resolution remains limited.

Second, our validation is based on spatial consistency and order-of-magnitude plausibility rather than pixel-level accuracy (see Supplementary Discussion 2): we compare the geographic distribution of modelled risk against observed damage patterns from the July 2021 floods, and find broad agreement at the regional level (e.g. Rhineland-Palatinate and Wallonia identified as high-risk areas). The additional CEMS comparison provides an independent illustration of the spatial correspondence between flood evidence mapped during the 2021 event and the historical 100-year hazard map used in this analysis. Because the two datasets represent an event-specific observation and a probabilistic hazard layer, respectively, the comparison is not interpreted as a formal event-specific validation. A more direct pixel-level evaluation of the damage estimates would require spatially explicit post-event observations of building damage and material loss, potentially derived from high-resolution satellite imagery combined with detailed building information. Such observations would provide a valuable event-specific reference for assessing the spatial distribution and order-of-magnitude plausibility of the estimated impacts, while complementing the EAD estimates, which represent probability-weighted annual averages across multiple return periods[13,14,52].

Future scenarios hold the spatial distribution and composition of the building-material stock layer constant and should therefore be interpreted as hazard-driven counterfactuals rather than complete projections of future flood impacts. Urban expansion and continued construction in flood-prone areas could increase future exposure, while zoning, managed retreat, building adaptation and changes in construction practices could reduce or redistribute it. Coupling the framework with spatially explicit dynamic building-stock scenarios would allow future changes in exposure and material composition to be represented. Similarly, the emissions calculations retain present-day material production intensities. Decarbonisation of electricity, cement, steel and other material supply chains would reduce the emissions associated with a given quantity of replacement material. Consequently, the projected material demand reflects the assumed evolution of hazard under fixed exposure, while the long-term emissions estimates are conditional on current production emission factors.

Another important source of uncertainty concerns the translation from building-level monetary damage to material replacement. The applied functions distinguish residential, commercial and industrial buildings but do not represent differences in the flood vulnerability of individual materials and components. Structural concrete and steel may remain largely in place after inundation, whereas timber elements, insulation, plasterboard, interior finishes and building services may require more extensive replacement. The model may therefore overestimate replacement of some structural materials while underrepresenting damage to more vulnerable components that are not separately resolved in the material stock dataset. Developing material- and component-specific vulnerability functions linked to building typology, construction system and flood duration would substantially improve future estimates.

Finally, the reconstruction pathway represented in this study is intentionally linear, translating replacement equivalent damage into an equal mass of newly produced material. Actual recovery may combine partial repair, refurbishment, selective component replacement, direct reuse, recycling and substitution with lower carbon

materials. These pathways could reduce virgin material demand and embodied emissions, although their feasibility may be constrained by contamination, mixed debris, structural safety requirements, limited temporary storage and the urgency of post-disaster reconstruction. Our results should therefore be interpreted as gross replacement equivalent demand before circular recovery rather than realised production under a specific reconstruction strategy. Post-disaster sorting and storage capacity, pre-established recovery protocols and procurement systems for secondary materials could make circular reconstruction an important component of both climate adaptation and emissions mitigation.

Methods

We develop GloBUME-Flood[53], a spatial assessment framework combining building material stocks, probabilistic riverine and coastal flood depth maps, and subnational flood protection standards to estimate material exposure, replacement equivalent material demand and associated cradle-to-gate GHG emissions. The spatial and computational workflow is summarised in Supplementary Figs. 1 and 2. We outline each database and model used further below.

Flood mapping for different climate scenarios

We use riverine and coastal flood maps from the Aqueduct Floods Hazard dataset (updated October 20, 2020)[34,54]. The dataset provides information on the extent and depth of riverine and coastal floods, gridded to 30″ (roughly 1 km at the equator). The maps are developed using the GLOFRIS flood hazard modelling approach, originally developed for river floods by (43) and Ward et al.[55] and extended for future flooding (Ward et al.[25]; Winsemius et al.[56]) and coastal flooding (Tiggeloven et al.[26]). It provides probabilistic flood-hazard layers for baseline conditions (2010) and future projected climate conditions in 2030, 2050 and 2080, based on averages over 40-year windows centered around these years. These simulations include several return periods (2, 5, 10, 25, 50, 100, 250, 500 and 1000 years). Future climate conditions are projected based on RCP 4.5 and RCP 8.5. Future riverine flood hazards are distinguished by five global climate models (GCM): HadGEM2-ES, IPSL-CM5A-LR, MIROC-ESM-CHEM, GFDL-ESM2M and NorESM1-M. Land subsidence is included. The dataset represents some of the best open-source information on the impact of future climate changes on riverine and coastal flood hazards on a global level[25,57]. Representative national maps of the historical riverine and coastal flood depth inputs are provided for Belgium and Germany in Supplementary Fig. 7.

Building material stocks

Material stocks of buildings used in this study are derived from ref. 29. The material dataset provides the mass of six types of building materials (concrete, steel, aluminium, copper, glass, wood; distinguished by residential and non-residential uses) located in each Nighttime Light Cell (NLC) across Europe. NLCs are distinctly shaped cells of variable sizes that capture individual human settlements by identifying isolated patches of light, surrounded by areas with no or less nighttime lights. These NLCs are thus data-driven spatial units of human activity, independent of formal administrative boundaries. The smallest NLC is composed of a single pixel of 0.1 km. Building material stocks are held at their current spatial distribution and quantities in all future scenarios. Future changes in modelled impacts therefore isolate changes in flood hazard and effective protection rather than changes in socioeconomic exposure. Representative spatial distributions of concrete, steel, wood, aluminium, copper and glass stocks are shown for Belgium and Germany in Supplementary Fig. 6.

Calculation of material exposure

Here, material exposure is calculated as the mass of material stocks impacted by floods, that is, materials located in a flooding area where inundation depth exceeds 0 m. First, we calculate the gridded inundated areas that intersect with building material stocks. To prevent double counting, overlapping pixels from riverine and coastal floods are counted as a single event. All spatial datasets were standardised to the WGS84 geographic coordinate system (EPSG:4326) prior to overlay analysis. The building material polygons (NLCs) were reprojected to WGS84 where necessary, and the flood raster point grids were confirmed to share the same coordinate reference system before intersection. Material quantities were then allocated to flood pixels proportionally based on the area of overlap between each polygon and pixel.

Calculation of maximum potential material damages

A fraction of materials exposed to flood hazards may be damaged. Maximum potential material damages in floods can be evaluated by combining impacted material mass and inundation depth values that are further translated into a damage percentage via the flood depth–damage functions (see Supplementary Figs. 1 and 2 for schematic diagrams). The flood depth–damage functions in this analysis are derived from ref. 58, a globally consistent database depicting fractional monetary damage function of water depth across continents and building classes (residential, commercial and industrial buildings). A further disaggregation between the material stock data (residential and non-residential) and the depth–damage function classes (residential, commercial and industrial) is necessary. Following the literature[54], we assume that non-residential building material stocks consist of 60% commercial and 40% industrial building materials. We acknowledge that applying standard depth–damage functions to estimate material replacement at shallow flood depths (e.g. <0.5 m) may overestimate damage, as minor inundation does not necessarily require full material replacement. The functions used here assign zero damage below 0.5 m inundation depth, providing a minimum threshold. Nevertheless, the assumption that damaged materials are fully replaced on a one-to-one basis may not hold for all flood depths and building types. This represents a conservative upper-bound estimate of material demand and associated emissions; actual reconstruction may involve partial repairs rather than full replacement, particularly for shallow floods.

The depth–damage functions distinguish building use but not material type. We therefore apply the same building-class damage fraction to each material within the corresponding residential or non-residential stock and interpret the resulting mass as replacement-equivalent material demand. This is a modelled proxy rather than a direct observation of material-specific physical damage.

Calculation of expected annual material damages

Different return periods (2, 5, 10, 25, 50, 100, 250 and 1000 years) of flood hazards represent different annual average exceedance probabilities (i.e. 1/return periods). Each impact indicator (e.g. material exposure, maximum potential material damage) is calculated per return period (probability). By considering the material damage of flooding over the full range of probabilities, flood risk can be further measured as the expected average annual damage (EAD) of building materials from flood hazards[59]. EAD is calculated using the damage-probability curve, where the flood probabilities (i.e. 1/return periods) are plotted on the x-axis, and the maximum material damages on the y-axis (Supplementary Fig. 3). The area or the integral under the curve is the EAD (before incorporating flood protections; see the following paragraph). Future EADs are calculated for each of the five GCMs, and the reported values in this study are the average. EAD is computed using the trapezoidal rule, with weights $w_1 = (p_1 - p_2)/2$ for the shortest return period, $w_i = (p_{i-1} - p_{i+1})/2$ for interior points ($i = 2,\ldots,8$), and $w_9 = (p_8 - p_9)/2 + p_9$ for the longest return period, where the final term assumes flood depth remains constant beyond the 1-in-1000-year event. Throughout this study, material damage refers to estimated

replacement demand derived using the depth–damage functions rather than directly observed physical damage to material stocks.

We independently calculate damages from riverine and coastal flooding events and then combine these figures to estimate the overall damages. However, the combined total is not entirely accurate, as it does not reflect the dynamic interactions between these flood types, where one type can exacerbate or mitigate the effects of another[60]. Future improvements could involve the use of more sophisticated models or data to better simulate the complex interactions between these flood types.

Material damage from flood hazards can be reduced with infrastructure such as dikes. We account for flood protection standards by introducing a vertical flood protection line[54] to the damage-probability curve, which truncates the overall area under the curve into two areas showing the protected/avoided (i.e. the area to the left of the flood protection line) and the unprotected/expected (i.e. the area to the right of the flood protection line) damages. That is, the represented damage to the right of the flood protection line is assumed as avoided (and set to zero). Current flood protection standards are derived from the model layer of the FLOPROS database for river and for coastal[26,31] both of which provide state-level flood protection estimates across the globe, expressed as return periods in years (e.g. 100 years). More recent Europe-specific datasets[61] infer empirical protection levels from historical flood occurrence and impact data, which are valuable for analysing observed flood impacts and vulnerability. However, these empirical protection metrics reflect the combined effects of structural protection, exposure, vulnerability and reporting patterns, rather than the physical design standard of flood defences alone. We therefore retain FLOPROS as the protection input for this analysis. We then estimate future protection standards for current dike heights under different climate change and land subsidence scenarios, assessing how risks evolve when existing dikes and infrastructure are physically maintained. Future protection standards in the scenario of maintaining dike heights, but not upgrading, are derived by mapping future (climate-driven, no socioeconomic) risk with current risks associated with return periods between 2 and 1000, linearly interpolated.

Calculation of material-related emissions

Material-related GHG emissions are calculated by multiplying estimated material damage, interpreted here as replacement-equivalent material demand, by the material-specific GHG emission factors (i.e. emissions per kg of materials production). To estimate the corresponding requirement for new material production, we assume a one-to-one replacement ratio between the replacement-equivalent material demand and the mass of new materials produced. That is, the same mass and categories of building materials are assumed to be produced to restore the affected building stock. This assumption represents a transparent, like-for-like reconstruction benchmark and does not account for partial repair, refurbishment, direct reuse, recycled material inputs or material substitution. The estimates therefore represent gross replacement requirements under this benchmark before potential reductions from material recovery and alternative reconstruction pathways. Cumulative material demand and embodied emissions over 2024–2080 were calculated by piecewise linear interpolation of the annual values between the baseline, 2050 and 2080, followed by integration over the study period. The GHG emission factors for each material are derived from the Ecoinvent 3.6 database[62], employing the global warming potential (with a 100-year time horizon) approach, and the 'cradle-to-gate' material production system boundary (referring to only the production of materials, from raw material extraction to the manufacturing of finished products). Transportation, on-site construction, and other pre-use phase activities are not included in this analysis due to their relatively small contributions and inconsistent data availability[63]. Material production emission factors are held constant across all years and scenarios to isolate the effect of changing flood hazard. Future emission estimates therefore represent the emissions associated with replacement under present-day production intensities rather than forecasts of future material production systems. See detailed emissions factors in Supplementary Table 4.

Uncertainty analysis

We quantified uncertainty from two distinct sources: (1) climate model (GCM) ensemble spread in future flood projections, and (2) sensitivity to the choice of depth–damage functions. For the first source, each future riverine scenario was driven by five GCM members (HadGEM2-ES, IPSL-CM5A-LR, MIROC-ESM-CHEM, GFDL-ESM2M and NorESM1-M); we report the ensemble mean alongside the 5th–95th percentile range (p05–p95) across members for each country-material combination (Supplementary Fig. 4). For the historical baseline, a single climate forcing is available, and ensemble statistics are not applicable. For coastal flooding, the flood model applies a single sea-level rise projection per scenario, so within-scenario GCM spread is zero; coastal uncertainty is instead characterised by the difference between RCP4.5 and RCP8.5 projections. To summarise spatial heterogeneity in GCM uncertainty, we computed the coefficient of variation ($CV = \sigma/\mu$) per country by aggregating ensemble standard deviations across material types in quadrature and dividing by the summed ensemble mean. For the second source, we compared our baseline JRC depth–damage curves[58] with an alternative set from the Rhine Atlas developed by the International Commission for the Protection of the Rhine (ICPR)[64]. The ICPR curves assign lower damage fractions at shallow inundation depths (<2 m) and converge with the Huizinga curves at deeper inundation (>4 m). EU-total EAD and embodied GHG emissions under the ICPR curves are around 10% lower than the JRC baseline for future scenarios, and approximately 20% lower for the historical baseline where shallow river floods dominate. These differences do not alter the main conclusions of the study. Results of this sensitivity analysis are presented in Supplementary Fig. 5.

Reporting summary

Further information on research design is available in the Nature Portfolio Reporting Summary linked to this article.

Data availability

The input datasets used in this study are publicly available from the original sources cited in the Methods and Supplementary Information. The derived model outputs underlying the reported results and figures are available in the Zenodo archive[53] at: https://doi.org/10.5281/zenodo.23094216. Source data are provided with this paper.

Code availability

The Python code used for spatial preprocessing, model calculations, analysis, and figure generation is archived on Zenodo[53] at: https://doi.org/10.5281/zenodo.23094216.

References

1. Mallapaty, S. Why are Pakistan's floods so extreme this year? *Nature* https://doi.org/10.1038/d41586-022-02813-6 (2022).
2. Szczyrba, L. Hurricane damage harms the most vulnerable, reveals inequality and social divides. *Queen's Gazette* https://www.queensu.ca/gazette/stories/hurricane-damage-harms-most-vulnerable-reveals-inequality-and-social-divides (2021).
3. Mohr, S. et al. A multi-disciplinary analysis of the exceptional flood event of July 2021 in central Europe. Part 1: event description and analysis. *Nat. Hazards Earth Syst. Sci. Discuss.* **2022**, 1–44 (2022).
4. Central Europe: Floods—Sep 2024 https://reliefweb.int/disaster/fl-2024-000169-aut (2024).
5. West and Central Africa: Floods 2024 https://reliefweb.int/topic/west-and-central-africa-floods-2024 (2024).

6. Iglesias, V. et al. Risky development: increasing exposure to natural hazards in the United States. *Earths Future* **9**, e2020EF001795 (2021).
7. Tellman, B. et al. Satellite imaging reveals increased proportion of population exposed to floods. *Nature* **596**, 80–86 (2021).
8. *The Human Cost of Disasters: An Overview of the Last 20 Years (2000-2019)* https://www.undrr.org/publication/human-cost-disasters-overview-last-20-years-2000-2019 (UNDRR, 2020).
9. Koks, E. E. et al. A global multi-hazard risk analysis of road and railway infrastructure assets. *Nat. Commun.* **10**, 2677 (2019).
10. Hirabayashi, Y. et al. Global flood risk under climate change. *Nat. Clim. Change* **3**, 816–821 (2013).
11. Alfieri, L. et al. Global projections of river flood risk in a warmer world. *Earths Future* **5**, 171–182 (2017).
12. Nicholls, R. J. et al. A global analysis of subsidence, relative sea-level change and coastal flood exposure. *Nat. Clim. Change* **11**, 338–342 (2021).
13. Blöschl et al. Changing climate shifts timing of European floods. *Science* **357**, 588–590 (2017).
14. Blöschl et al. Changing climate both increases and decreases European river floods. *Nature* **573**, 108–111 (2019).
15. Rentschler, J., Salhab, M. & Jafino, B. A. Flood exposure and poverty in 188 countries. *Nat. Commun.* **13**, 3527 (2022).
16. Hallegatte, S., Vogt-Schilb, A., Bangalore, M. & Rozenberg, J. *Unbreakable: Building the Resilience of the Poor in the Face of Natural Disasters* (World Bank Publications, 2016).
17. *UK Climate Change Risk Assessment: Government Report 2012*. *GOV.UK* https://www.gov.uk/government/publications/uk-climate-change-risk-assessment-government-report.
18. Watkiss, P., Cimato, F., Hunt, A. & Morley, B. *Climate Change Impacts on the Future Cost of Living*, SSC/CCC004 (Joseph Rowntree Foundation, 2016).
19. Dottori, F. et al. Increased human and economic losses from river flooding with anthropogenic warming. *Nat. Clim. Change* **8**, 781–786 (2018).
20. Willner, S. N., Otto, C. & Levermann, A. Global economic response to river floods. *Nat. Clim. Change* **8**, 594–598 (2018).
21. Vousdoukas, M. I. et al. Climatic and socioeconomic controls of future coastal flood risk in Europe. *Nat. Clim. Change* **8**, 776–780 (2018).
22. Tanoue, M., Taguchi, R., Alifu, H. & Hirabayashi, Y. Residual flood damage under intensive adaptation. *Nat. Clim. Change* **11**, 823–826 (2021).
23. Wing, O. E. J. et al. Inequitable patterns of US flood risk in the Anthropocene. *Nat. Clim. Change* **12**, 156–162 (2022).
24. Jongman, B. et al. Increasing stress on disaster-risk finance due to large floods. *Nat. Clim. Change* **4**, 264–268 (2014).
25. Ward, P. J. et al. A global framework for future costs and benefits of river-flood protection in urban areas. *Nat. Clim. Change* **7**, 642–646 (2017).
26. Tiggeloven, T. et al. Global-scale benefit-cost analysis of coastal flood adaptation to different flood risk drivers using structural measures. *Nat. Hazards Earth Syst. Sci.* **20**, 1025–1044 (2020).
27. Haberl, H. et al. High-resolution maps of material stocks in buildings and infrastructures in Austria and Germany. *Environ. Sci. Technol.* **55**, 3368–3379 (2021).
28. Tanikawa, H. & Hashimoto, S. Urban stock over time: spatial material stock analysis using 4d-GIS. *Build. Res. Inf.* **37**, 483–502 (2009).
29. Peled, Y. & Fishman, T. Estimation and mapping of the material stocks of buildings of Europe: a novel nighttime lights-based approach. *Resour. Conserv. Recycl.* **169**, 105509 (2021).
30. Donati, F. et al. The future of artificial intelligence in the context of industrial ecology. *J. Ind. Ecol.* **26**, 1175–1181 (2022).
31. Scussolini, P. et al. FLOPROS: an evolving global database of flood protection standards. *Nat. Hazards Earth Syst. Sci.* **16**, 1049–1061 (2016).
32. Zhong, X. et al. Global greenhouse gas emissions from residential and commercial building materials and mitigation strategies to 2060. *Nat. Commun.* **12**, 6126 (2021).
33. Thieken, A. H. et al. Performance of the flood warning system in Germany in July 2021–insights from affected residents. *Nat. Hazards Earth Syst. Sci.* **23**, 973–990 (2023).
34. Winsemius, H. C., Van Beek, L. P. H., Jongman, B., Ward, P. J. & Bouwman, A. A framework for global river flood risk assessments. *Hydrol. Earth Syst. Sci.* **17**, 1871–1892 (2013).
35. Willner, S. N., Levermann, A., Zhao, F. & Frieler, K. Adaptation required to preserve future high-end river flood risk at present levels. *Sci. Adv.* **4**, eaao1914 (2018).
36. Endendijk, T. et al. Experience from the 2021 floods in the Netherlands: household survey results on impacts and responses. *J. Coast. Riverine Flood Risk* **2** (2023).
37. Aerts, J. C. J. H. A review of cost estimates for flood adaptation. *Water* **10**, 1646 (2018).
38. Lo, W. et al. Evaluation of flood mitigation effectiveness of nature-based solutions potential cases with an assessment model for flood mitigation. *Water* **13**, 3451 (2021).
39. Tiggeloven, T. et al. The benefits of coastal adaptation through conservation of foreshore vegetation. *J. Flood Risk Manag.* **15**, e12790 (2022).
40. Satellite imaging reveals increased proportion of population exposed to floods. *Nature* https://www.nature.com/articles/s41586-021-03695-w.
41. The Next American Migration: What Cities Should Know About Climate Change and Populations on the Move. *National League of Cities* https://www.nlc.org/resource/the-next-american-migration-what-cities-should-know-about-climate-change-and-populations-on-the-move/ (2022).
42. Poorly Planned Urban Development as a Risk Driver of Disaster https://www.preventionweb.net/understanding-disaster-risk/risk-drivers/poorly-planned-urban-development (2021).
43. Mortensen, E. et al. The potential of global coastal flood risk reduction using various DRR measures. *Nat. Hazards Earth Syst. Sci.* **24**, 1381–1400 (2024).
44. Chester, M. V., Underwood, B. S. & Samaras, C. Keeping infrastructure reliable under climate uncertainty. *Nat. Clim. Change* **10**, 488–490 (2020).
45. Hawkesbury-Nepean Floodplain Management Steering Committee. *Reducing Vulnerability of Buildings to Flood Damage: Guidance on Building in Flood Prone Areas* (Hawkesbury-Nepean Floodplain Management Steering Committee, 2006).
46. Abdelhafez, M. A., Ellingwood, B. & Mahmoud, H. Hidden costs to building foundations due to sea level rise in a changing climate. *Sci. Rep.* **12**, 14020 (2022).
47. Kreibich, H., Thieken, A. H., Petrow, T., Müller, M. & Merz, B. Flood loss reduction of private households due to building precautionary measures–lessons learned from the Elbe flood in August 2002. *Nat. Hazards Earth Syst. Sci.* **5**, 117–126 (2005).
48. Phonphoton, N. & Pharino, C. A system dynamics modeling to evaluate flooding impacts on municipal solid waste management services. *Waste Manag.* **87**, 525–536 (2019).
49. Amato, A. et al. Disaster waste management after flood events. *J. Flood Risk Manag.* **13**, e12566 (2020).
50. Brown, C., Milke, M. & Seville, E. Disaster waste management: a review article. *Waste Manag.* **31**, 1085–1098 (2011).
51. Vousdoukas, M. I. et al. African heritage sites threatened as sea-level rise accelerates. *Nat. Clim. Change* **12**, 256–262 (2022).

52. Bertola, M. et al. Megafloods in Europe can be anticipated from observations in hydrologically similar catchments. *Nat. Geosci.* **16**, 982–988 (2023).
53. Zhong, X. GloBUME-Flood: modelling flood-related building material demand and greenhouse gas emissions. Preprint at https://doi.org/10.5281/ZENODO.23094216 (2026).
54. Ward, P. J. et al. *Aqueduct Floods Methodology* https://www.wri.org/research/aqueduct-floods-methodology (2020).
55. Ward, P. J. et al. Assessing flood risk at the global scale: model setup, results, and sensitivity. *Environ. Res. Lett.* **8**, 044019 (2013).
56. Winsemius, H. C. et al. Global drivers of future river flood risk. *Nat. Clim. Change* **6**, 381–385 (2016).
57. Trigg, M. A. et al. The credibility challenge for global fluvial flood risk analysis. *Environ. Res. Lett.* **11**, 094014 (2016).
58. Huizinga, J., de Moel, H. & Szewczyk, W. *Global Flood Depth-Damage Functions: Methodology and the Database with Guidelines* https://doi.org/10.2760/16510 (2017).
59. Meyer, V., Haase, D. & Scheuer, S. Flood risk assessment in European river basins—concept, methods, and challenges exemplified at the Mulde River. *Integr. Environ. Assess. Manag.* **5**, 17–26 (2009).
60. Wang, S., Najafi, M. R., Cannon, A. J. & Khan, A. A. Uncertainties in riverine and coastal flood impacts under climate change. *Water* **13**, 1774 (2021).
61. Paprotny, D., t Hart, C. M. P. & Morales-Nápoles, O. Evolution of flood protection levels and flood vulnerability in Europe since 1950 estimated with vine-copula models. *Nat. Hazards* **121**, 6155–6184 (2025).
62. Wernet, G. et al. The ecoinvent database version 3 (part I): overview and methodology. *Int. J. Life Cycle Assess.* **21**, 1218–1230 (2016).
63. United Nations Environment Programme. *2021 Global Status Report for Buildings and Construction* https://www.unep.org/resources/report/2021-global-status-report-buildings-and-construction (United Nations Environment Programme, 2021).
64. Messner, F. et al. *Evaluating Flood Damages: Guidance and Recommendations on Principles and Methods* (2007).

Acknowledgements

We thank Arnold Tukker for helpful discussions and insightful comments on the manuscript.

Author contributions

X.Z. conceived the study, developed the analytical framework, conducted the analysis, produced the visualisations and drafted the manuscript. P.B. contributed to the research design, framing and interpretation of the results. T.F., T.T., Y.P., Y.J. and P.J.W. contributed to the interpretation of the results and revision of the manuscript. X.Z., T.F., T.T., Y.P., Y.J., P.J.W. and P.B. reviewed and edited the manuscript and approved the final version.

Funding

This work was supported by the start-up fund of Tsinghua University Shenzhen International Graduate School. P.B. acknowledges funding from the British Academy Global Professorships.

Competing interests

The authors declare no competing interests.

Additional information

Supplementary information The online version contains Supplementary Material available at https://doi.org/10.1038/s41467-026-79185-2.

Correspondence and requests for materials should be addressed to Xiaoyang Zhong.

Peer review information *Nature Communications* thanks Lorenzo Alfieri and the other, anonymous, reviewer(s) for their contribution to the peer review of this work. A peer review file is available.

Reprints and permissions information is available at http://www.nature.com/reprints

Publisher's note Springer Nature remains neutral with regard to jurisdictional claims in published maps and institutional affiliations.

Open Access This article is licensed under a Creative Commons Attribution 4.0 International License, which permits use, sharing, adaptation, distribution and reproduction in any medium or format, as long as you give appropriate credit to the original author(s) and the source, provide a link to the Creative Commons licence, and indicate if changes were made. The images or other third party material in this article are included in the article's Creative Commons licence, unless indicated otherwise in a credit line to the material. If material is not included in the article's Creative Commons licence and your intended use is not permitted by statutory regulation or exceeds the permitted use, you will need to obtain permission directly from the copyright holder. To view a copy of this licence, visit http://creativecommons.org/licenses/by/4.0/.

© The Author(s) 2026

This Article in Press is shared early to give you faster access to new research. It is citable and carries a permanent DOI. The final edited version will replace it automatically.